Title
ENERGY DISPERSIVE X-RAY FLUORESCENCE SPECTROMETRY FOR DETERMINATION OF TWENTY-SIX TRACE AND TWO MAJOR ELEMENTS IN GEOCHEMICAL SPECIMENS

Author
Giauque, Robert D.

Publication Date
1976-07-01

Submitted to Analytical Chemistry

LBL-5212 Rev.
Preprint

ENERGY DISPERSIVE X-RAY FLUORESCENCE SPECTROMETRY FOR DETERMINATION OF TWENTY-SIX TRACE AND TWO MAJOR ELEMENTS IN GEOCHEMICAL SPECIMENS

Robert D. Giauque, Roberta B. Garrett, and
Lilly Y. Goda

July 1976

Prepared for the U. S. Energy Research and
Development Administration under Contract W-7405-ENG-48

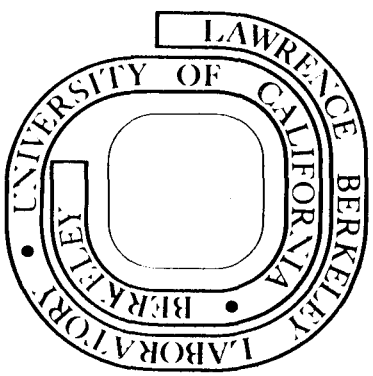

DISCLAIMER

LBL-5212
Rev.

ENERGY DISPERSIVE X-RAY FLUORESCENCE SPECTROMETRY FOR DETERMINATION OF TWENTY-SIX TRACE AND TWO MAJOR ELEMENTS IN GEOCHEMICAL SPECIMENS

Robert D. Giauque,* Roberta B. Garrett, and Lilly Y. Goda

Energy and Environment Division
Lawrence Berkeley Laboratory
University of California
Berkeley, California 94720

July 1976

BRIEF

The concentrations of twenty-eight elements in pulverized geochemical specimens are determined within twenty minutes. Accuracies of 5% or better are typically obtained. The intensity of the Compton scattered excitation radiation serves as an internal standard and is used to ascertain corrections required to compensate for matrix absorption effects. Calibration is achieved using geochemical reference standards.

*denotes corresponding author

To be submitted to Analytical Chemistry

LBL-5212
Rev.

ENERGY DISPERSIVE X-RAY FLUORESCENCE SPECTROMETRY FOR DETERMINATION OF TWENTY-SIX TRACE AND TWO MAJOR ELEMENTS IN GEOCHEMICAL SPECIMENS

Robert D. Giauque, Roberta B. Garrett, and Lilly Y. Goda

Energy and Environment Division
Lawrence Berkeley Laboratory
University of California
Berkeley, California 94720

ABSTRACT

A method for analyzing geochemical specimens by energy dispersive x-ray fluorescence is described. In our method we make use of the fact that at any given x-ray energy between adjacent major element absorption edges, both the reciprocal of the specimen mass absorption coefficient and the spectral background intensity vary linearly with the intensity of the Compton scattered excitation radiation. Hence, Compton scattered excitation radiation serves a dual role: (1) as an internal standard and (2) as a measure of spectral background intensity. Several pure compounds, for which the x-ray cross sections vary over a wide range, are used to develop individual x-ray line spectral background curves. Standardization is achieved utilizing geochemical reference standards. Accuracies typically obtained are 5% or better using twenty minute analysis periods.

LBL-5212
Rev.

INTRODUCTION

In the field of geochemistry, a technique which permits rapid and accurate multielement analysis with a minimum of cost and sample preparation effort is often desired. In this paper we demonstrate that x-ray induced energy dispersive x-ray fluorescence analysis (XRFA) easily lends itself to the determination of twenty-six trace and two major elements in geochemical specimens. Approximately 2 gm of powdered specimen pressed into a cylinder is used for analysis. Accuracies of 5% or better are typically obtained using twenty minute analysis periods.

The XRFA technique requires the excitation and detection of characteristic K or L x-ray lines of the individual elements within the specimen that are to be determined. For very thin specimens, x-ray line intensities, counts/sec, vary linearly with elemental concentration. However, for thick specimens, x-ray line intensities are not usually linear with concentration because of matrix absorption and enhancement effects. Some of the methods which have been used to minimize and compensate for matrix absorption and enhancement effects are discussed elsewhere in the literature (1-2).

Reynolds (3-4) has shown that the Compton scattered excitation radiation peak intensity and the mass absorption coefficient are inversely related for infinitely thick specimens. Both Reynolds (3) and Feather and Willis (5) have used this fact to compensate for matrix absorption effects for the determination of the elements Ni (Z=28) through Zr (Z=40) in geochemical specimens. In each case wavelength dispersive XRFA was the technique used.

In this paper we demonstrate that the approach used by both Reynolds (3) and Feather and Willis (5) is applicable to energy dispersive XRFA and

can easily be extended to include the determination of the elements Ti (Z=22) through Fe (Z=26) and Pd (Z=46) through Ba (Z=56).

DISCUSSION OF METHOD

Background of Method. Andermann and Kemp (6) were the first to show that scattered x-rays could be used as an internal standard in XRFA. Reynolds (3) and, more recently, Feather and Willis (5) have used the intensity of the Compton scattered excitation radiation to correct for matrix absorption effects in analysis of trace amounts of the elements Ni (Z=28) through Zr (Z=40) in geochemical specimens. In their method, advantage is taken of the fact that the intensity of the Compton scattered radiation varies linearly with the reciprocal of the mass absorption coefficient between adjacent major element absorption edges. Since Fe is typically the highest atomic number major constituent present in geochemical specimens, individual specimen mass absorption coefficient curves vary smoothly over energies greater than 7.1 keV, the Fe K absorption edge energy. These investigators have also shown that the intensity of the spectral background, for each of the element characteristic x-ray lines within this range, varies linearly with the intensity of the Compton scattered excitation radiation. They used infinitely thick pure materials, for which the x-ray mass absorption coefficient varied over a wide range, to relate spectral background to Compton scattered radiation intensity. Using this procedure, individual element spectral background curves were established. Hence, the Compton scattered excitation radiation serves a dual role: (1) as an internal standard to compensate for matrix absorption effects and (2) as a measure of the intensities of the spectral background for individual elements to be determined.

Reynolds (4) has also reported using a series of simultaneous equations to calculate mass absorption coefficients for some of the elements, Ti (Z=22) through Fe (Z=26), which have x-ray lines of energies less than 7.1 keV, the Fe K absorption edge. However, in his analytical approach, matrix enhancement effects are neglected.

General Technique for Obtaining X-ray Spectra. Figure 1 is a schematic of our XRFA system. Radiation provided by an x-ray tube is used to excite characteristic x-rays from elements within the specimen. These x-rays along with scattered excitation radiation are simultaneously measured by the detector. Since detection system count rate limitations, generally around 10,000 counts/sec, are often easily attained, near monochromatic excitation radiation is frequently utilized to achieve high peak to background ratios for x-rays excited from a given range of elements.

Preparation of Specimen. Specimens initially should be pulverized until the particle diameters are smaller than one-fifth the effective penetration depth for the measured x-ray energy to minimize the possibility of mineralogical effects (7). For many geochemical specimens this corresponds to a size of 10-50 microns when analyzing for elements down to Ti (Z=22). Approximately 2 gm of powder is pressed at a pressure of 8,000 psi into a lucite cylinder, 2.5 cm O.D., 1.27 cm I.D., and 1.3 cm high, as shown in Figure 2. The specimen is contained by Scotch tape (No. 302) on the bottom.

Equipment and Characteristics. A guard-ring detector with pulsed light feedback electronics and a 512 channel pulse height analyzer were used for the analytical determinations. The total resolution of the system, FWHM,

was 225 eV at 6.4 keV (Fe Kα x-ray energy) at 5,000 counts/sec using an 18 μsec pulse peaking time. Excitation was provided by a Mo transmission x-ray tube with a combined anode plus window thickness of 0.010 cm. The x-ray tube was operated at 42 kV with regulated currents varying from 100-300 μA when analyzing for the elements Ti-Zr. For the determination of the elements Pd-Ba, the x-ray tube was operated at 48 kV and a 0.010 cm Mo filter was inserted externally to the x-ray tube. Using this procedure spectral backgrounds were reduced substantially compared to individual x-ray line intensities, since the exciting Bremstrahlung radiation was shifted to higher energies with a maximum intensity at 38 keV.

The distances between the x-ray tube anode and the specimen, and between the specimen and the detector were approximately 6 and 2.5 cm, respectively. The angles formed by the exciting and the detected emergent radiations with the specimen surface were both near 45°. The total specimen volume that is in direct line with both the excitation and detection radiation beams is shown in Figure 1. For analysis, the spectral data acquired were recorded on magnetic tape. Computations were made using a Control Data 6600 computer. Our program requires less than 50 K of core space.

CALIBRATION METHOD

Spectrum Background. The background under each of the x-ray lines that are used for analysis is referred to as the spectral background. Curves, which relate the intensity of the spectral background to the intensity of the Compton scattered excitation radiation, were established for x-ray lines from each of the elements to be determined using five powdered materials, MgO, Al_2O_3, NaSCN, KH_2PO_4, and S. These were chosen since they have mass

absorption coefficients which cover the range of most geochemical specimens. Additionally, in most cases, they were free of measurable impurities. Figure 3 shows the spectral background curve established for nickel. This curve illustrates the relationship between the intensity of the Compton scattered excitation radiation, the reciprocal of the mass absorption coefficient of the specimen for Ni Kα x-rays, and the intensity of the spectral background. Similar background curves were established for each of the elements determined. The background counts obtained from each material were all normalized to the same counting period and x-ray tube current. (In order to minimize the possibility of a minor base line or gain shift, backgrounds were determined using essentially constant data acquisition rates by varying the x-ray tube current.)

The intensity of the spectral background at the intercept which corresponds to zero Compton scattered excitation radiation intensity is referred to as the residual background and, most likely, is due to system scattering (e.g., scattering from air and the Scotch tape window). It is thought that the nonzero intercept for $1/\mu$ is related to the residual background. The portion of the spectral background which is above the residual background is the true background as described by Feather and Willis (5). It is this portion of the spectral background which is linearly related to both the intensity of the Compton scattered excitation radiation and the reciprocal of the mass absorption coefficient. Thus, for analysis, individual spectral backgrounds may be ascertained directly from the intensity of the Compton scattered excitation radiation. This radiation should be in an energy range that is free from any significant contribution by specimen element x-rays.

For the elements Ti-Zr, linear curves which relate the intensity of the spectral background to the intensity of the Compton scattered Mo Kα radiation were established. For the elements Pd-Ba, spectral background intensities were linearly related to Bremstrahlung scattered radiation (between 26 and 30 keV) intensity. (This energy range of Bremstrahlung scattered radiation contained a minor fraction of coherent scattered radiation. In the geometry employed for analysis, between 1.5 and 2.0 keV is lost by the Compton scattering process in the energy range of Bremstrahlung used. Consequently, the energy range utilized minimized the contribution of coherent scattered radiation.)

Overlapping X-ray Background. Our analysis program uses a fixed number of channels for each element to be determined. Peak overlaps were initially established from thin deposits of each element, which were prepared by nebulization of solutions of individual elements onto Nuclepore polycarbonate filters, or by dusting the element or appropriate compound onto tape.

Since x-ray mass absorption coefficient values increase with decreasing x-ray energy, thick specimens have characteristic x-ray line ratios (e.g., Kβ/Kα) which deviate from the ratios ascertained using thin deposits of each element. These deviations were calculated, as they take on values equal to the ratios of the reciprocal of the mass absorption coefficients for the individual x-ray lines. Mass absorption coefficient curves have been calculated for each of the six geochemical reference specimens that were used for standardization. Figure 4 illustrates three of these curves. Mass absorption coefficient data reported by McMaster et al. (8) and major element concentration data reported by Flanagan (9) and Perlman and

Asaro (10) were used for the calculations. For the different matrices, calculated reciprocal mass absorption coefficient ratios for characteristic x-ray lines (e.g., Kβ/Kα) from any one element were found to be constant to within ±0.5%.

Additional minor corrections were made to these ratios to compensate for the absorption by the Scotch tape window. These corrections were established by making transmission measurements using the Scotch tape as an absorber for the excitation and fluorescent radiations. Absolute calibration for overlap of L with K x-ray lines (e.g., Ba L x-rays with Ti, V, Cr, and Mn K x-rays) was determined using nebulized standard solution deposits (11).

Standardization. Elements with Characteristic X-rays of Energies Greater than 7.1 keV. Typically, Fe is the highest atomic number major constituent element present in geochemical specimens. Mass absorption coefficient curves are linear over energy ranges greater than 7.1 keV, the Fe K absorption edge energy, as illustrated in Figure 4. As previously shown in Figure 3, the intensity of the true background is directly proportional to the reciprocal of the mass absorption coefficient. Thus, element concentration is linearly related to the ratio of the spectral peak intensity to the true background.

Calibration for the analysis of the elements Ni, Cu, Zn, Ga, As, Rb, Sr, Y, Zr, Ba, and Pb was accomplished using five USGS geochemical reference standards, AGV-1, BCR-1, DTS-1, PCC-1, and G-2 (9) and Standard Pottery (10). Linear calibration curves, some of which are illustrated in Figure 5, were established. The determination of the true background is the key to the method used to compensate for matrix absorption effects.

Calibration for Cd, Sn, Sb, and Cs was achieved using a multielement synthetic glass standard, VS-N (12). Using the response of the x-ray system to the analysis of nearby elements, calibration for Ge, Se, Br, Pd, Ag, In, Te, and I was accomplished by interpolation.

Standardization. Elements with Characteristic X-rays of Energies Less than 7.1 keV. As illustrated in Figure 4, there is an abrupt change in the total mass absorption coefficient curves for the geochemical reference specimens at 7.1 keV, the Fe K absorption edge, as Fe is a major constituent. Hence, using the spectrum background procedure previously described, true background intensity, determined for each of the elements with characteristic x-rays of energies less than 7.1 keV, is directly proportional to the reciprocal of apparent total mass absorption coefficient, μ_{app}. The value of μ_{app} does not reflect the drop in the curve at 7.1 keV and may be obtained from the curve--extrapolated to energies less than 7.1 keV. The difference between the true value of μ and the value of μ_{app} is equal to the weight fraction of Fe present, multiplied by the difference between μ and μ_{app} for pure Fe at the specific energy.

Linear curves, which relate values of μ_{app} with the ratio of the total (true + residual) to the true spectrum background, were established for each of the elements Ti, V, Cr, Mn, and Fe. Values for μ_{app} were calculated for each of the geochemical reference standards using major element concentration and total mass absorption coefficient data reported in the literature (8-10). The ratio of the total to the true spectrum background for Ti, V, Cr, Mn, and Fe were determined experimentally for each of the standards. Figure 6 illustrates the linear curve established for Fe Kα

x-rays which relates the ratio of the total to the true spectrum background to μ_{app}.

For analysis, the initial weight fraction results determined for Fe were adjusted by iteration ten times using Equation 1.

$$W_i = \left(\frac{\mu_{app} - \Delta\mu \cdot W_j}{\mu_{app}} \right) W_o \qquad (1)$$

where

μ_{app} is the apparent total mass absorption coefficient at the Fe Kα x-ray energy.

W_i, W_j, and W_o are the new, present, and initial weight fractions, respectively.

$\Delta\mu$ is the difference between the extrapolated and the true cross section for pure Fe at the Fe Kα x-ray energy.

In effect, initial weight fraction values determined for Fe, which are uncorrected for the drop in the mass absorption curve at 7.1 keV, are corrected by iteration during which the ratio of the true μ to μ_{app} is calculated.

For the elements Ti-Mn, the values ascertained for W_o were adjusted once using Equation 1. For these calculations the determined weight fraction of Fe, corrected for matrix absorption effects, was used for W_j. The value assigned for $\Delta\mu$ was the difference between the extrapolated and the true cross section for pure Fe at the Kα x-ray energy of the individual element. The apparent total mass absorption coefficient for the Kα x-ray of interest is μ_{app}.

Additional first order corrections were made for the elements Ti-Mn to compensate for matrix enhancement by the Fe K x-rays. The cross section

of the geochemical specimens for the exciting Mo K radiation was a magnitude less than that for the Fe K x-rays. Hence, the intensity of the Fe K radiation was treated as being essentially constant across the specimen depth from which Ti-Mn K x-rays were measured. Utilizing physical data reported in the literature (8, 13-14), corrections for matrix enhancement by Fe K x-rays were made using Equation 2.

$$W_i' = W_i \left[1 - \left(\frac{\tau_i \cdot W_i}{\mu_{app} - \Delta\mu \cdot W_{Fe}} \right) \omega_i \cdot f_i \cdot \frac{I_{Fe\ K\alpha}}{I_{i\ K\alpha}} \cdot R \right] \qquad (2)$$

where

W_i and W_i' are the weight fraction of element i corrected for matrix absorption and for matrix absorption plus enhancement, respectively.

μ_{app} is the apparent total mass absorption coefficient of the specimen at energy $i_{K\alpha}$.

W_{Fe} is the weight fraction of Fe corrected for matrix absorption.

τ_i is the photoelectric mass absorption coefficient of element i for Fe Kα x-rays.

ω_i is the K fluorescence yield for element i.

f_i is the fraction of Kα to total K x-rays emitted from element i.

$\Delta\mu$ is the difference between the extrapolated and the true Fe cross section at energy i Kα.

$I_{Fe\ K\alpha}$ and $I_{i\ K\alpha}$ are the spectral Kα line intensities determined for Fe and element i.

R is a constant which accounts for enhancement by both Fe Kα and Kβ x-rays and also corrects for the difference in their cross sections.

For the elements Ti-Cr, R has a value of 1.10. For Mn, R has a value of 0.10 since only Fe Kβ x-rays will cause enhancement effects.

In effect, the fraction of the total mass absorption coefficient contributed by the photoelectric cross section for element i at the Fe Kα x-ray energy is approximated and expressed by the term within the parentheses in Equation 2. The product of $\omega_i \cdot f_i$ is the fraction of x-rays absorbed by element i which give rise to the emission of Kα x-rays. Multiplying the term within the parentheses by the product of $\omega_i \cdot f_i \cdot I_{\text{Fe K}\alpha}$ yields a first approximation of the total detected Kα x-rays of element i that are produced as a result of enhancement by Fe Kα x-rays. The term R corrects for enhancement by both Fe Kα and Kβ x-rays, and also corrects for the difference in the cross sections for these two x-ray energies.

RESULTS

To illustrate the capability of the method, four French geochemical reference standards were analyzed using the previously described equipment. Each of the standards was prepared in quintuplicate. Corrections for any slight deviation in the x-ray tube output or the excitation radiation-specimen-detector geometry were established daily using a 227 $\mu g/cm^2$ thin-film copper standard. Such deviations could have a small effect upon the residual background fraction of the total spectrum background ascertained for the individual spectral lines. Concentrations were calculated using Equation 3.

$$ppm_i = \frac{I_i}{tbkg_i} \cdot slope_i \qquad (3)$$

where

I_i is the spectral x-ray intensity from element i.

$tbkg_i$ is the true background intensity determined for element i.

$slope_i$ is the slope of the standard curve for element i.

The results are shown in Tables I-IV. Total analysis time for each specimen was twenty minutes. The errors listed are two standard deviations. For the elements which were determined to be below our detection limits, three standard deviations for counting statistics are reported. The neutron activation values listed were determined by F. Asaro and co-workers at this laboratory. The reported values are from the literature (15,16). Proposed values are listed in parentheses. As shown, the values ascertained are in good agreement with NAA and results reported in the literature. Typically, accuracies of 5% or better are obtained.

Figures 7 and 8 show the spectra obtained on Granite GA. Spectral background for the elements with K x-rays in the range of 31 to 32 keV (Cs, Ba) contain a fraction of coherent scattered excitation radiation, which causes larger errors in the determination of these elements. These errors could essentially be eliminated and much higher x-ray line/spectral background intensity ratios realized for these elements by operating the x-ray tube at approximately 60 kV and inserting a thicker external Mo filter. Doing so would shift the scattered radiation to higher energies. However, our excitation system is limited to a maximum voltage of 50 kV.

Using 100 mg specimens pressed into 0.32 cm I.D. cylinders, we have calibrated the system and determined the concentrations of elements with characteristic x-rays of energies less than 16 keV. To do so required highly collimated excitation and detection radiation beams. Sensitivities realized were approximately a factor of 2 less than those attained with 2 gm specimens. Although the results obtained were dependent upon the density of the prepared specimens, typically accuracies of 10% or better were achieved.

ACKNOWLEDGMENTS

The authors thank Frank Asaro, Helen Michel, and Harry Bowman for providing the French geochemical reference standards and the neutron activation analysis data. We are grateful to them and to Joe Jaklevic and Carl Blumstein for their comments on the preparation of this paper.

CREDIT

This work was done with support from the U.S. Energy Research and Development Administration. Any conclusions or opinions expressed in this report represent solely those of the author(s) and not necessarily those of the Lawrence Berkeley Laboratory nor of the U.S. Energy Research and Development Administration.

LITERATURE CITED

1. H.A. Liebhafsky, H.G. Pfeiffer, E.H. Winslow, and P.D. Zemany, "X-rays, Electrons, and Analytical Chemistry. Spectrochemical Analysis with X-rays," Wiley-Interscience (1972).
2. L.S. Birks, "X-ray Spectrochemical Analysis," Wiley-Interscience (1969).
3. R.C. Reynolds, Jr., Amer. Mineral 48, 1133 (1963).
4. R.C. Reynolds, Jr., Amer. Mineral 52, 1493 (1967).
5. C.E. Feather and J.P. Willis, X-ray Spect. 4, 41 (1976).
6. G. Andermann and J.W. Kemp, Anal. Chem. 30, 1306 (1958).
7. R. Jenkins, "An Introduction to X-ray Spectrometry," Heyden (1974).
8. W.H. McMaster, N.K. Del Grande, J.H. Mallett, and J.H. Hubbell, "Compilation of X-ray Cross Sections," Univ. of Calif., Lawrence Livermore Lab. Report UCRL-50174, Section II, Revision I (1969).
9. F.J. Flanagan, Geochim. Cosmochim. Acta 37, 1189 (1973).
10. I. Perlman and F. Asaro, in Science and Archaeology, R.H. Brill, ed., MIT Press (1971).
11. R.D. Giauque, R.B. Garrett, and L.Y. Goda, "Calibration of Energy Dispersive X-ray Spectrometers for Analysis of Thin Environmental Samples," Lawrence Berkeley Lab. Report LBL-4481 (1976).
12. Etude Cooperative, Analusis 2, 59 (1973).
13. W. Bambynek, et al., Rev. of Mod. Phys. 44, 716 (1972).
14. J.S. Hansen, H.U. Freund, and R.W. Fink, Nucl. Phys. A142, 604 (1970).
15. M. Roubault, H. de La Roche, and K. Govindaraju, Sci. de La Terre, Tome XV, 4, 351 (1970).
16. H. de La Roche and K. Govindaraju, Bull. de la Soc. Francaise de Ceramique 85, 35 (1969).

Table I. Analysis of Granite GA

	X-ray Fluorescence	Neutron Activation	Reported
Ti	0.226%±.014	0.174%±.042	0.228%
V	<160ppm	—	36ppm
Cr	<51ppm	7.4ppm±2.6	(10)ppm
Mn	712ppm±33	631ppm±16	665ppm
Fe	1.94%±.08	1.95%±.06	1.98%
Ni	<8ppm	<26ppm	7ppm
Cu	20ppm±8	—	14ppm
Zn	72ppm±7	76ppm±8	75ppm
Ga	15ppm±2	—	16ppm
Ge	<2ppm	—	(1.5)ppm
As	<3ppm	<4ppm	—
Se	<3ppm	—	—
Br	<3ppm	—	—
Pb	32ppm±2	—	—
Rb	180ppm±2	175ppm±12	175ppm
Sr	313ppm±4	—	305ppm
Y	21ppm±2	—	(18)ppm
Zr	123ppm±11	—	140ppm
Pd	<5ppm	—	—
Ag	<5ppm	—	—
Cd	<4ppm	—	—
In	<5ppm	—	—
Sn	<6ppm	—	(4)ppm
Sb	<7ppm	<0.20ppm	—
Te	<9ppm	—	—
I	<11ppm	—	—
Cs	19ppm±15	6.6ppm±0.4	(5)ppm
Ba	840ppm±37	816ppm±36	850ppm

Table II. Analysis of Basalt BR

	X-ray Fluorescence	Neutron Activation	Reported
Ti	1.57%±.04	1.64%±.05	1.57%
V	175ppm±86	—	240ppm
Cr	310ppm±44	379ppm±10	420ppm
Mn	1587ppm±36	1521ppm±36	1600ppm
Fe	9.13%±.09	9.10%±.22	9.01%
Ni	232ppm±12	281ppm±41	270ppm
Cu	80ppm±11	—	70ppm
Zn	151ppm±12	171ppm±16	160ppm
Ga	17ppm±3	—	(20)ppm
Ge	<3ppm	—	—
As	<3ppm	5.5ppm±3.2	—
Se	<3ppm	—	—
Br	<3ppm	—	—
Pb	6ppm±4	—	(16)ppm
Rb	43ppm±2	36ppm±25	45ppm
Sr	1326ppm±9	—	1350ppm
Y	35ppm±2	—	(27)ppm
Zr	259ppm±25	—	240ppm
Pd	<7ppm	—	—
Ag	<6ppm	—	—
Cd	<6ppm	—	—
In	<6ppm	—	—
Sn	<7ppm	—	(8)ppm
Sb	<8ppm	0.28ppm±.26	—
Te	<11ppm	—	—
I	<14ppm	—	—
Cs	<30ppm	0.65ppm±.50	—
Ba	1288ppm±84	1095ppm±50	1050ppm

Table III. Analysis of Diorite DR-N

	X-ray Fluorescence	Neutron Activation	Reported
Ti	0.57%±.02	0.62%±.04	0.67%
V	168ppm±126	—	225ppm
Cr	<60ppm	31.8ppm±4.6	45ppm
Mn	1785ppm±51	1640ppm±38	—
Fe	6.95%±.12	6.72%±.16	6.93%
Ni	<20ppm	38ppm±34	16ppm
Cu	44ppm±6	—	52ppm
Zn	144ppm±3	150ppm±14	150ppm
Ga	20ppm±2	—	(25)ppm
W	81ppm±11	—	—
As	3.7ppm±2.0	3.9ppm±2.6	—
Se	<3ppm	—	—
Br	<3ppm	—	—
Pb	55ppm±4	—	(75)ppm
Rb	70ppm±2	63ppm±22	(75)ppm
Sr	393ppm±3	—	400ppm
Y	29ppm±3	—	—
Zr	120ppm±14	—	—
Pd	<6ppm	—	—
Ag	<5ppm	—	—
Cd	4ppm±3	—	—
In	<6ppm	—	—
Sn	<6ppm	—	—
Sb	<8ppm	0.47ppm±.26	—
Te	<10ppm	—	—
I	<13ppm	—	—
Cs	<26ppm	6.2ppm±0.5	—
Ba	470ppm±35	380ppm±30	360ppm

Table IV. Analysis of Serpentine UB-N

	X-ray Fluorescence	Neutron Activation	Reported
Ti	0.035%±.011	0.042%±.015	0.07%
V	<100ppm	—	(100)ppm
Cr	2359ppm±47	2520ppm±60	2200ppm
Mn	1025ppm±24	971ppm±20	
Fe	6.14%±.06	5.83%±.14	5.96%
Ni	1907ppm±13	2113ppm±146	2000ppm
Cu	18ppm±4	—	(30)ppm
Zn	84ppm±3	107ppm±14	—
Ga	3.0ppm±1.1	—	—
Ge	2.1ppm±1.3	—	—
As	11ppm±2	12.4ppm±1.8	—
Se	<3ppm	—	—
Br	5ppm±2	—	—
Pb	11ppm±3	—	—
Rb	<3ppm	<24ppm	—
Sr	3ppm±2	—	(10)ppm
Y	<4ppm	—	—
Zr	<9ppm	—	—
Pd	<5ppm	—	—
Ag	<5ppm	—	—
Cd	<5ppm	—	—
In	<5ppm	—	—
Sn	<6ppm	—	—
Sb	<7ppm	0.28ppm±.24	—
Te	<9ppm	—	—
I	<12ppm	—	—
Cs	25ppm±15	11.3ppm±0.6	—
Ba	61ppm±21	32ppm±18	

FIGURE CAPTIONS

Fig. 1. Schematic of x-ray fluorescence analysis system.

Fig. 2. Apparatus used to prepare geochemical specimens.

Fig. 3. Spectral background curve established for nickel using five powdered materials. All background counts are normalized to 1000 sec count periods and an x-ray tube current of 100 μamps. (This curve also serves to illustrate that the Compton scattered excitation radiation intensity is directly proportional to both the true background and the reciprocal of the mass absorption coefficient.)

Fig. 4. Total mass absorption coefficient curves for reference standards BCR-1, AGV-1, and Standard Pottery.

Fig. 5. Standard curves which illustrate the relationship between concentration and the ratio of spectral line counts to true background.

Fig. 6. Apparent mass absorption coefficient curve established for Fe Kα x-rays using experimental spectrum/true background ratios and calculated apparent total mass absorption coefficients.

Fig. 7. X-ray spectrum obtained on Granite GA for the determination of the elements Ti-Zr.

Fig. 8. X-ray spectrum obtained on Granite GA for the determination of the elements Pd-Ba.

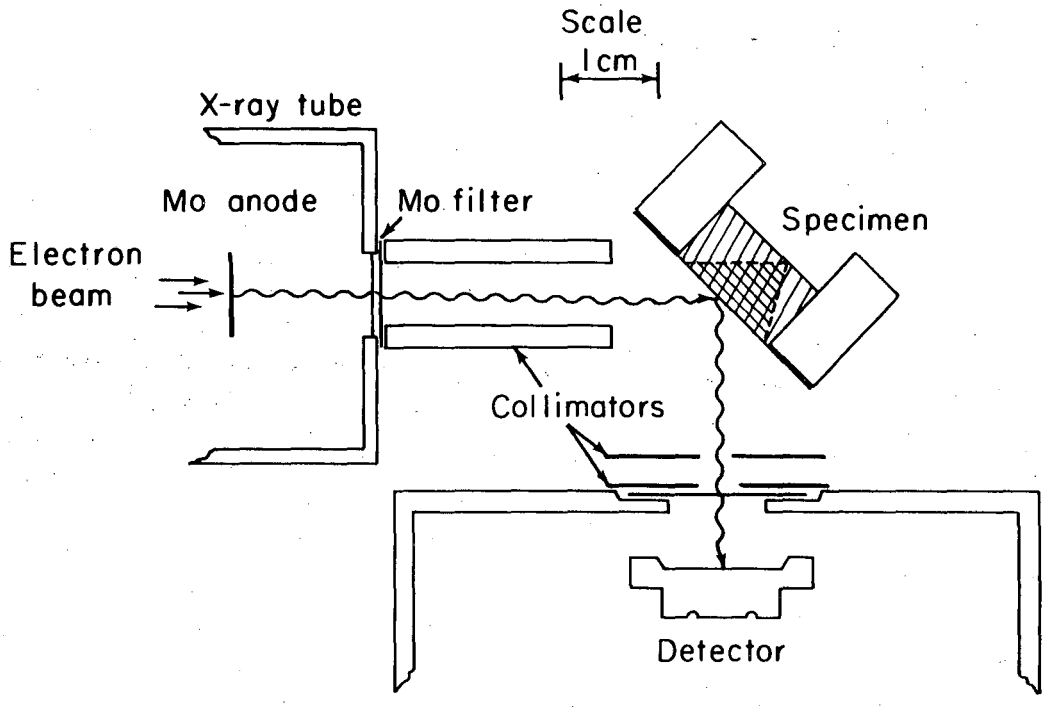

XBL 766 2928

Fig. 1

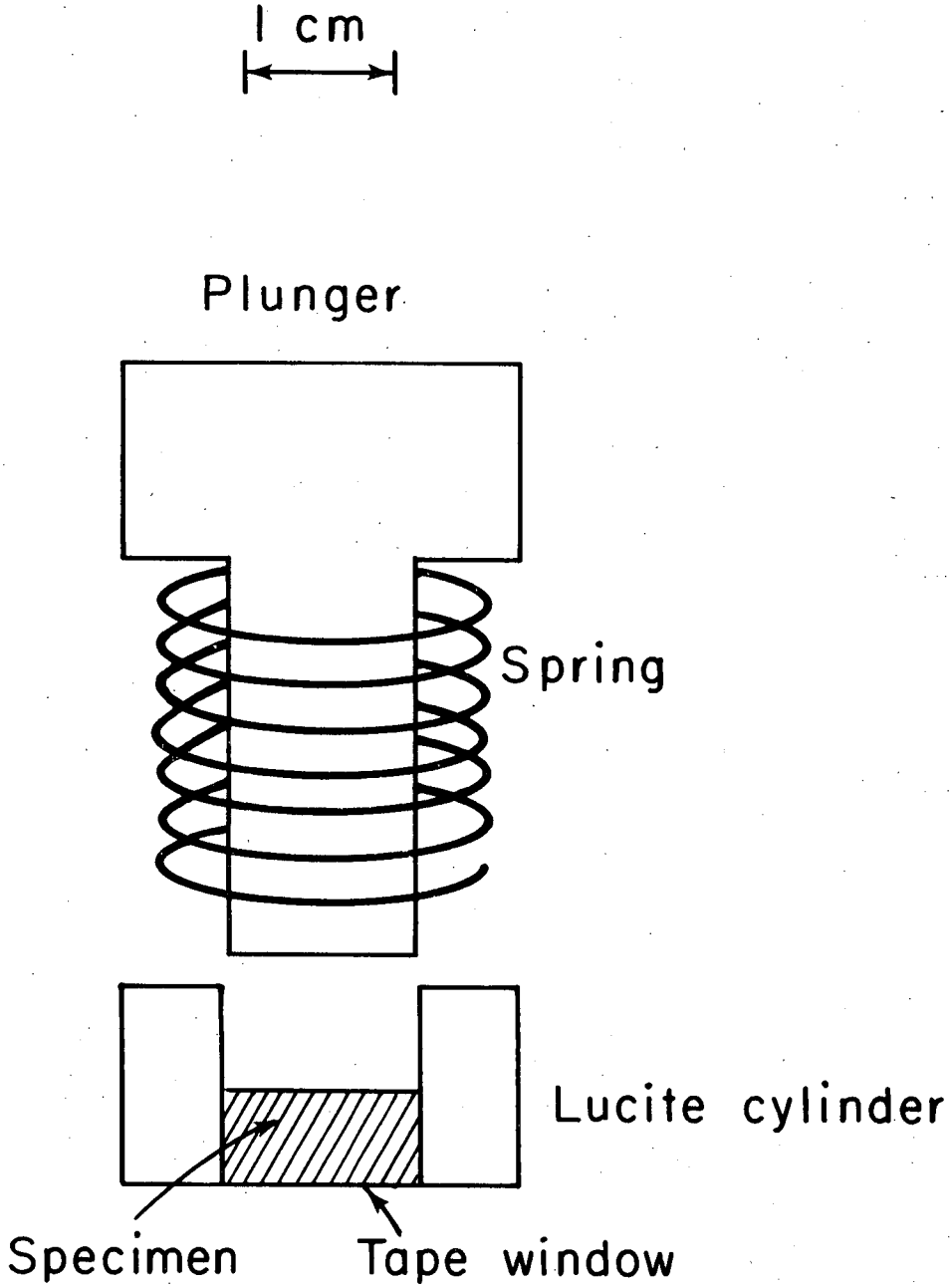

XBL 766-2927

Fig. 2

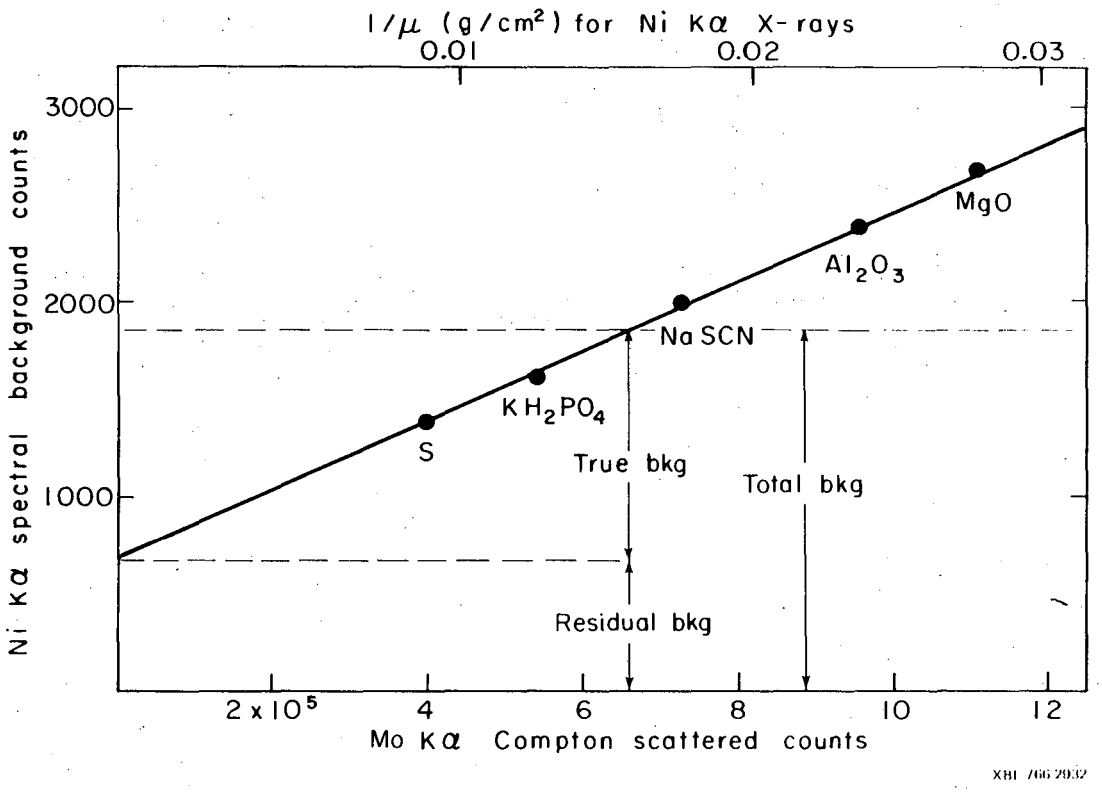

Fig. 3

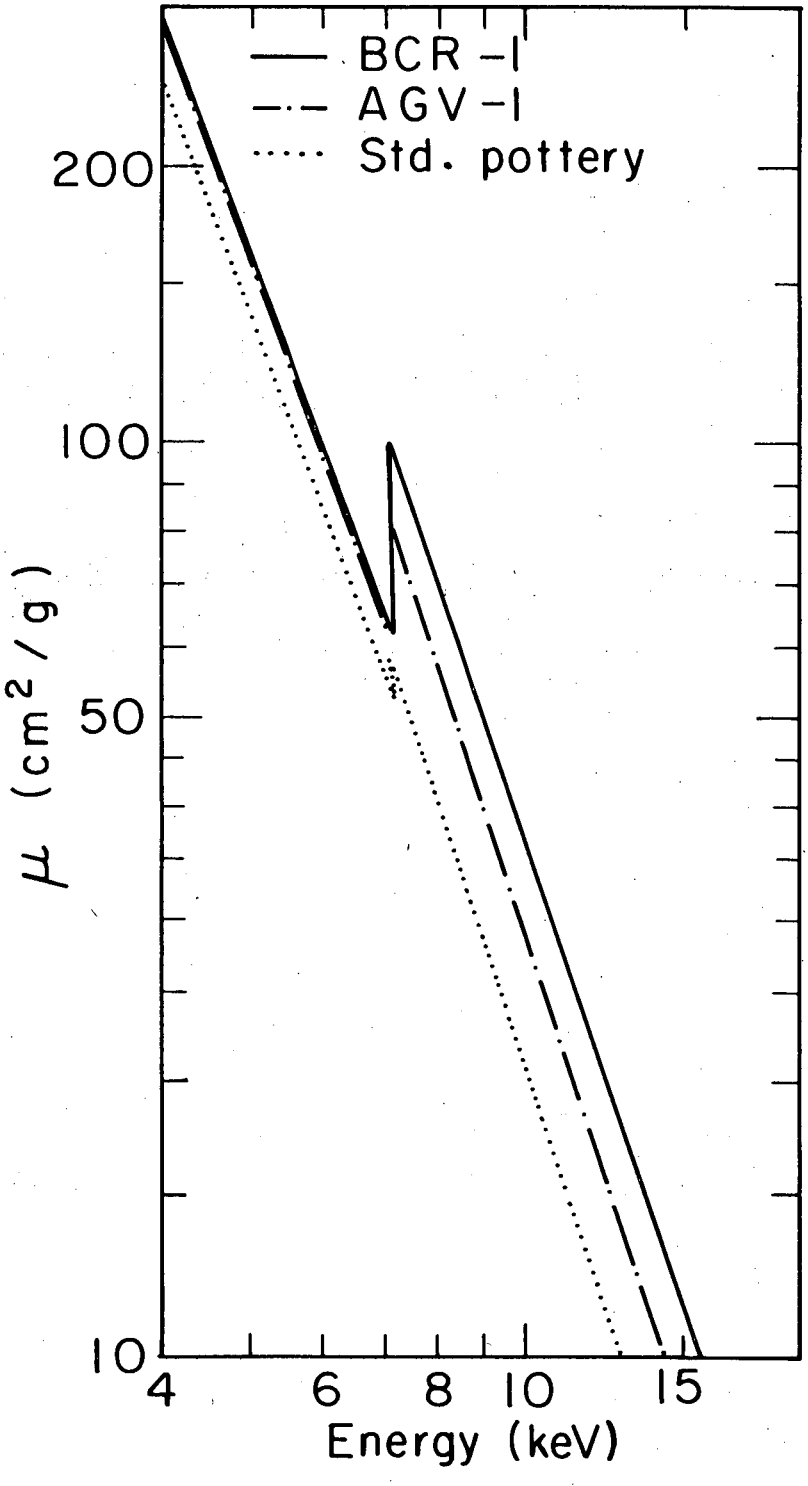

XBL 766 2930

Fig. 4

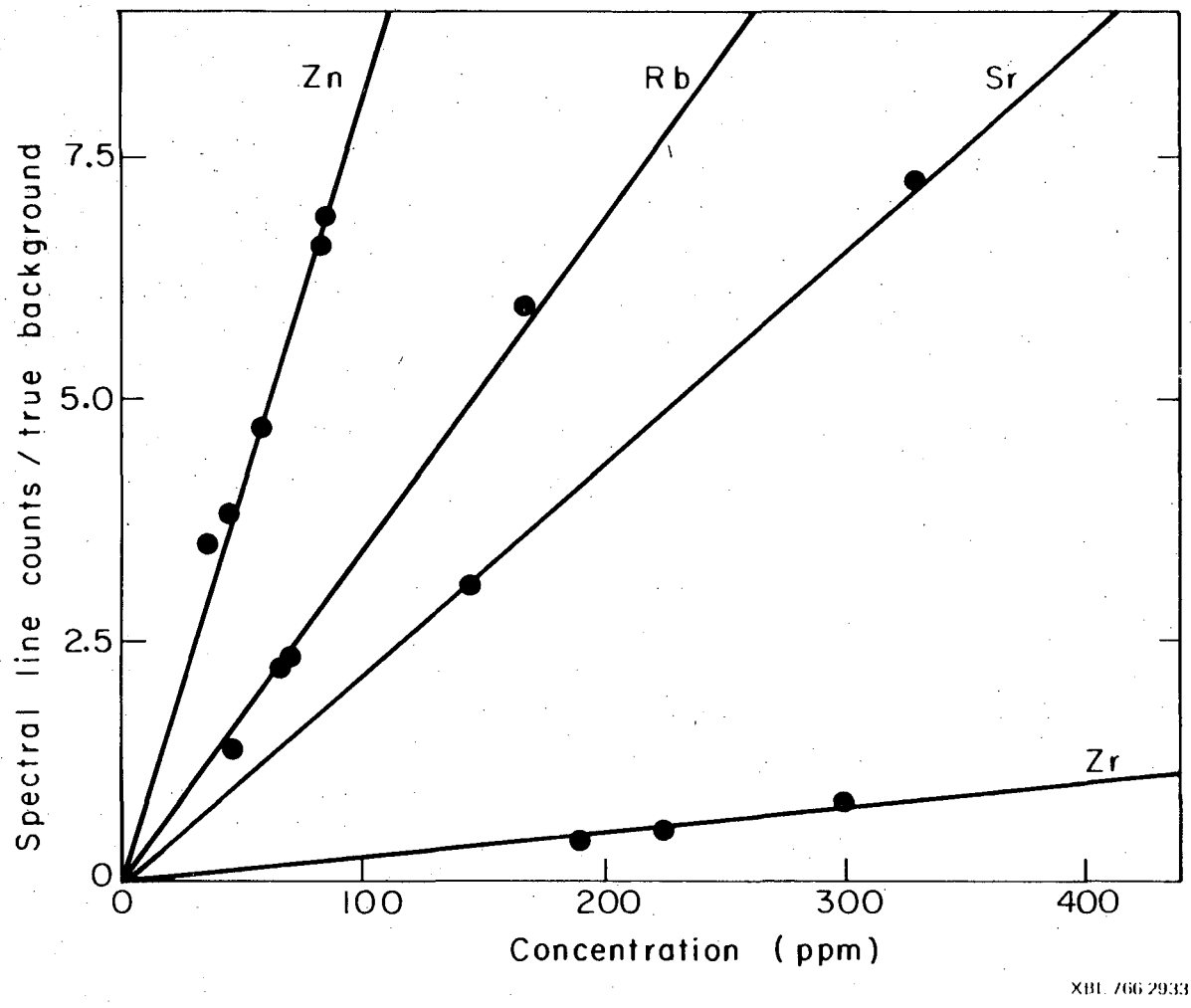

XBL 766 2933

Fig. 5

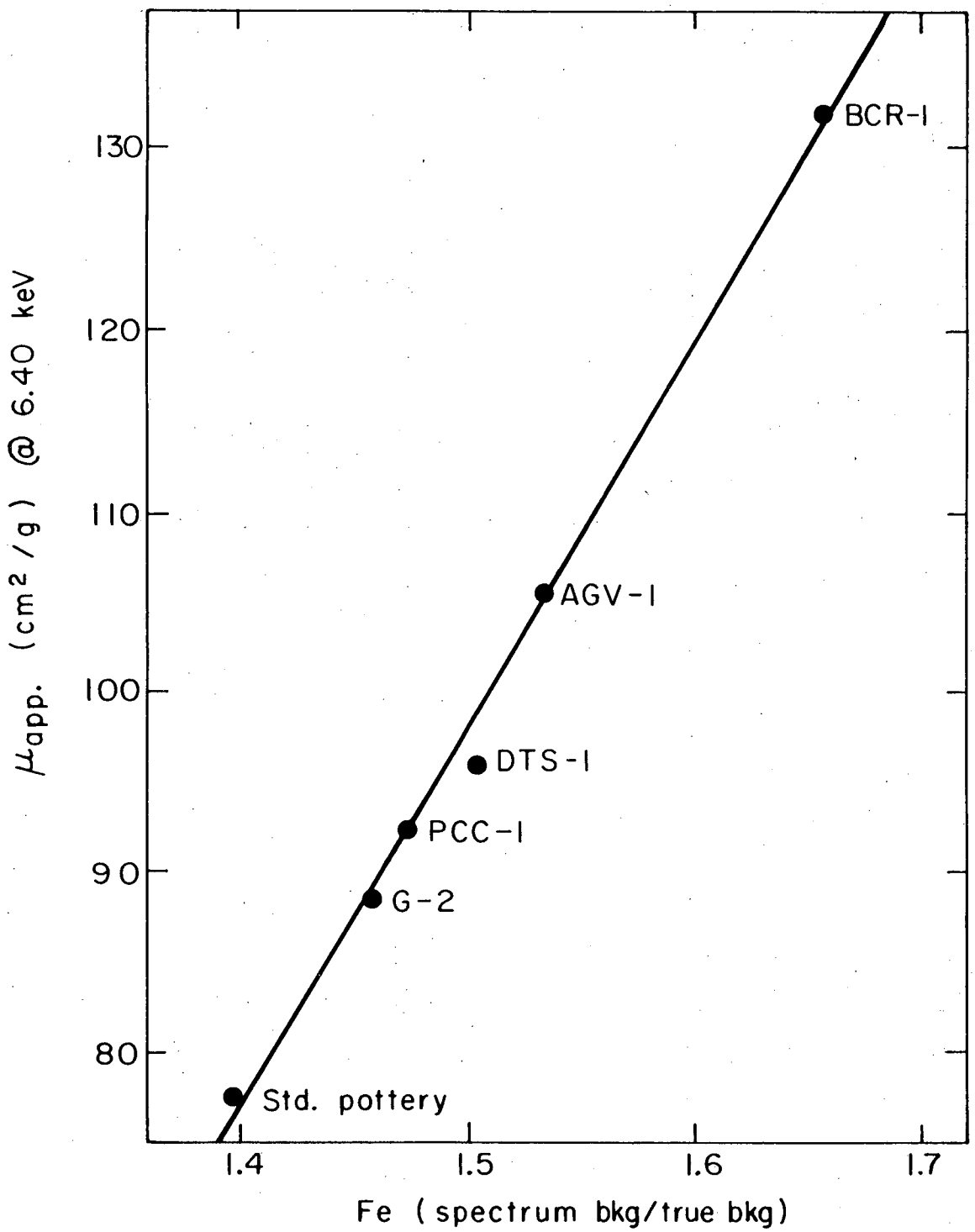

XBL 766 2929

Fig. 6

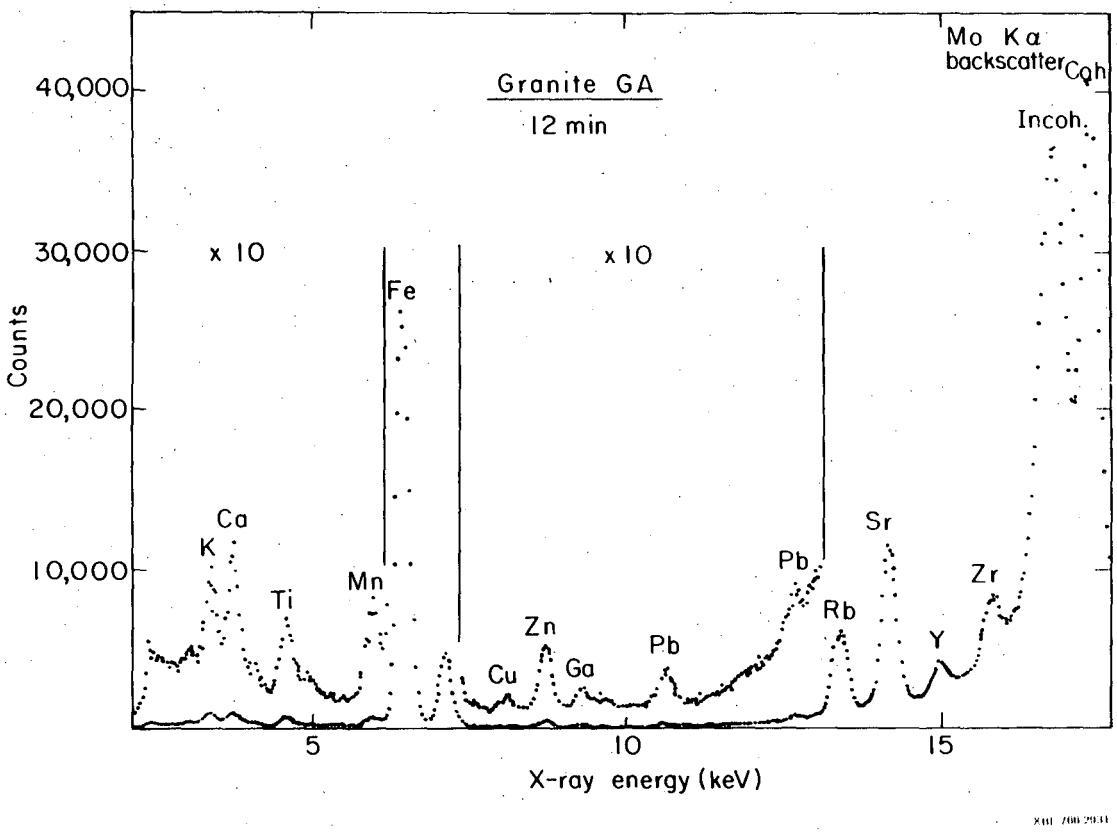

Fig. 7

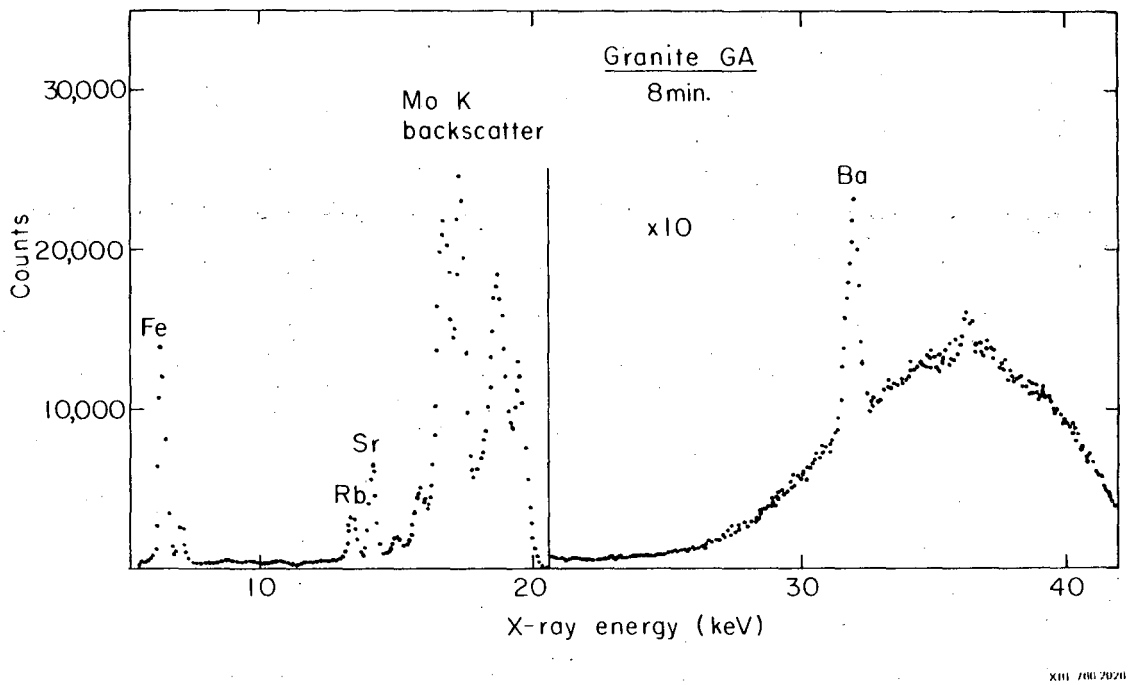
Granite GA
8min.
Mo K
backscatter
x10
Ba
Fe
Sr
Rb
Counts
30,000
20,000
10,000
10
20
30
40
X-ray energy (keV)

Fig. 8

This report was done with support from the United States Energy Research and Development Administration. Any conclusions or opinions expressed in this report represent solely those of the author(s) and not necessarily those of The Regents of the University of California, the Lawrence Berkeley Laboratory or the United States Energy Research and Development Administration.

TECHNICAL INFORMATION DIVISION
LAWRENCE BERKELEY LABORATORY
UNIVERSITY OF CALIFORNIA
BERKELEY, CALIFORNIA 94720